

Design of Hybrid-Electric Propulsion Systems for Small Unmanned Aerial Vehicles

*Joachim Schoemann and Mirko Hornung
Institute of Aircraft Design, Technische Universität München
Boltzmannstr. 15, 85747 Garching, Germany*

Abstract

Hybrid-electric propulsion systems are a combination of battery-electric and combustion engine propulsion systems. As such they have potential to combine the capability of silent flight with the capability of high velocity and long endurance flight phases. Existing design methods do not allow an accurate and generic sizing of these propulsion systems. Therefore, an accurate method based on power state variables that is generically applicable and requires low computational time is described in this paper. In comparison to conventional propulsion systems, the mass of hybrid-electric propulsion systems is highly dependent on the silent flight time. The main driver for mass is the battery.

1. Introduction

The term hybrid-electric propulsion system is not consistently used. It may generally be interpreted as a power plant in which various energy converters or energy storages are combined, of which at least one is electric. The objective is to advantageously consolidate the characteristics of the single components. In a hybrid fuel cell system for example, the fuel cell, characterized by high specific energy and relatively low specific power, is amended with a high specific power battery system. This addresses a typical dilemma in aircraft propulsion system design: The high power necessary for the short flight phase of takeoff sizes the power plant, whereas in the much longer cruise flight phase only a portion of the installed power is used and useless weight is carried in form of the heavy power plant. In a well-designed hybrid-electric propulsion system, the principal energy converter may be designed for cruise flight and be supported by an auxiliary one during takeoff and climb, or other high power demand flight phases.

Here, a hybrid-electric propulsion system is defined as the combination of internal combustion engine and battery-powered electric motor. In the automotive industry this system emerged into series production in the recent years, as it allowed lower fuel consumption than with conventional engines. Three factors contribute to a more fuel efficient system: The internal combustion engine mostly runs in its most efficient point of operation. At low power demand, excess power is charged into the batteries; at high power demand, additionally required power is supplied by the electric motor. At standstill or low speed, the engine is switched off, and the vehicle is propelled by the electric motor. During braking, energy is recuperated into the batteries.

In an aircraft, regenerative braking and frequent low speed or standstill phases are not applicable, because a flight mission is more static than a vehicle driving cycle. The use of the hybrid-electric propulsion system in aircraft offers the advantage of more silent flight. The noise caused by the internal combustion engine is eliminated when only the electric motor is running. Still it is not correct to speak of a generally quiet aircraft, as the propeller noise stays unaffected. Reducing the noise is especially advantageous for surveillance missions, one of the most common mission types of unmanned aircraft [1]. In those missions, very often the aircraft must operate covertly. A hybrid-electric aircraft combines the advantages of a silent electric aircraft with the elimination of one of its main disadvantages, the low endurance. During the flights to and from the target area noise is not a primary issue, so the hybrid-electric may perform these phases with high velocity and long endurance using the internal combustion engine and then electrically perform the surveillance phase. Furthermore the above mentioned propulsion system design dilemma may be solved by a dual-use of both machines during high power phases.

Another term in the title of this paper that requires definition is small unmanned aerial vehicles (UAV). A small UAV is here defined as a fixed-wing aircraft with a maximum takeoff mass (MTOM) of below 150 kg for operation in low altitudes. The hybrid-electric propulsion system with its capability of silent flight allows an aircraft to operate covertly in lower altitudes, which reduces the demands to the sensor payload and consequently allows a smaller and lower cost aircraft. The value of 150 kg signifies a current certification limit in Germany [2].

2. Problem statement

In this paper the potential of hybrid-electric propulsion systems shall be quantified by comparing them with two conventional propulsion technologies. As the references, the two systems the hybrid-electric one is composed of are considered as stand-alone systems: An internal combustion engine propulsion system and a battery-electric system. The three propulsion systems are compared over a wide range of requirements. For each set of requirements, each of the three systems is iteratively optimized. The method used to create these results is intended for future use in automated preliminary aircraft design. Three demands need to be met by a preliminary design method. In order to be used for varying requirements, with the given range up to 150 kg MTOM, the method needs to be generic. The use in preliminary design and for optimization requires a quick method with low computational effort. A further demand to every method used in preliminary aircraft design is accuracy.

High accuracy models may be obtained using state variables. State variables are the factors of power and may be divided into a flow and an effort variable [3]. Relevant couples for the propulsion system are, with the flow variables named first, velocity and force or rotational velocity and torque in the mechanical domain, current and voltage in the electrical domain, and mass flow and the lower heating value in the chemical domain. State variables allow the prediction of the efficiency of energy converters. In power based methods, in which a converter is assessed based only on its input or output power, this may not be done reliably and generically. To keep computational time low, it is important to avoid interpolation and file handling in the models. Interpolations may be replaced with surrogate models obtained with fits. Generality is assured by either validating models with a wide range of commercial products of the modeled component or by deriving the model from a respective database.

Published methods for the design of hybrid-electric propulsion systems are power based [9]. The reason for this is that they are used only for a certain use case, in which the designer may assume efficiencies. Publications also include very detailed simulation methods [4, 5], which are set-up for an already defined propulsion system and may not be used for the initial design of one. For fuel cell powered propulsion systems [6] or solar-electric system [7], methods based on state variables are available. Both methods discretely access databases of existing electric motors and other components, so that the demand of generality and low computational time are not fulfilled.

The method presented in this paper hence includes models based on state-variables for high accuracy, makes use of surrogate models for low computational effort and is based on extensive commercial off-the-shelf (COTS) databases to assure generality. It enables the preliminary design of hybrid-electric propulsion systems.

3. State-of-the-art of hybrid-electric propulsion systems

The only operative aircraft with hybrid-electric propulsion system the authors know of was developed and built at the Air Force Institute of Technology (AFIT) [8]. AFIT researchers previously published work on simulation and control of hybrid-electric propulsion systems [4], followed by a design method [9, 10] and propulsion system testing [11]. A team at the Queensland University of Technology set up a prototype of a parallel hybrid-electric propulsion system and evaluated the experimental performance [12, 13]. In further publications, the simulation and optimization of missions for hybrid-electric aircraft was investigated [5, 14]. Further projects on the design or construction of hybrid-electric propulsion systems are described in recently published work [15, 16, 17, 18]. The authors presented in [19] the method for the design of hybrid-electric propulsion systems, which is enhanced and used in this paper. Previous modifications and exemplary results are given in [20].

The hybrid-electric propulsion system shares components with other types of propulsion systems, so models may be taken from published work on those. The design and optimization of electric propulsion systems is described in [6] and [7]. In [6] the use case is a fuel cell system, whereas in [7] it is a solar-electric system. Both models use a discrete list of electric motors. The former work describes the only applicable model of motor controllers for brushless electric motors known to the authors. Experimental data on motor and controller efficiency is discussed in [21]. Generic approaches to the optimization of propeller-based propulsion systems are given in general [22] and for battery-electric propulsion systems in specific [23]. The former includes an approximation of internal combustion engine efficiency. More detailed approximation models for engine performance are available from automotive publications [3]. The influence of altitude on electric motor operation is described in [24].

4. Design process for hybrid-electric propulsion systems

Hybrid-electric propulsion systems exist in several configurations: The series configuration, the parallel configuration and the series-parallel configuration are the most common ones. The series configuration is characterized by a linear alignment of the components, as visible in the schematic diagram in Figure 1.

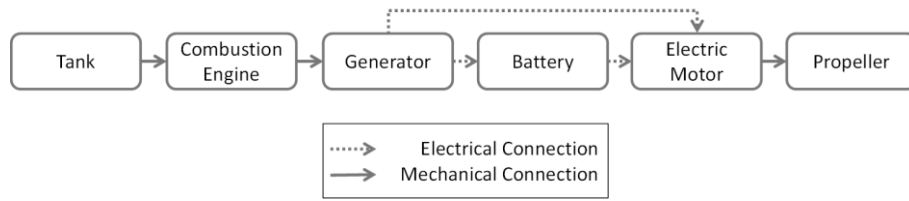


Figure 1: Series hybrid-electric configuration (modified from [19])

The propeller is driven by the electric motor, which draws energy from the battery. An internal combustion engine drives a generator, which may charge the battery or directly supply the electric motor. The clear disadvantage of this configuration is that the phenomenon described earlier as the propulsion design dilemma is not solved. The electric motor still needs to be sized for all flight phases and consequently is heavy. The generator also contributes to the system’s high mass. Furthermore, the fuel’s energy is converted so often, that its portion used for propelling the aircraft is very low.

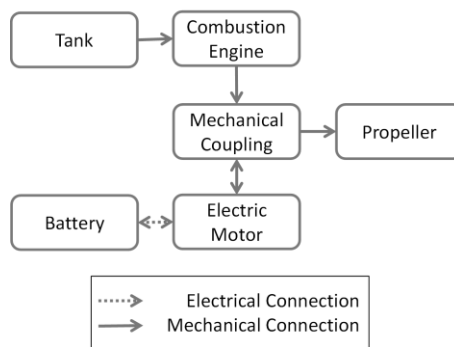


Figure 2: Parallel hybrid-electric configuration (modified from [19])

Figure 2 shows the parallel configuration, in which the propeller may be driven by the electric motor and the internal combustion engine. A coupling allows both plants to work singularly and in dual-mode. Dual-modes are either the concurrent drive of the propeller or the use of the electric motor as generator, which is then driven by the engine. Within the aircraft design process, the propulsion system design is fed with data on the demand in thrust, velocity and flight time to propel the aircraft during all mission phases. Its main output is the system mass. Aircraft Design is a highly iterative process, in which variations in mass affect the thrust requirement. The output of the propulsion system design module influences its input. A propulsion system design process hence should not be conducted isolated. On the other hand, aircraft design is a very complex process and requires the consideration of much more parameters than those related to the propulsion system. Therefore, here only the propulsion system design procedure is presented and used, as it allows clear identification and isolation of the influences of changes in the propulsion system.

In any propulsion system that consumes fuel, a constantly changing mass has to be considered when formulating the design requirements for the system. A common way to determine the fuel consumption accurately is a mission simulation. This however is an iterative and therefore time consuming method and requires information on the aircraft. In preliminary design, a flight mission is therefore divided into flight phases and a characteristic design point is defined for each. For each design point, the requirements to the propulsion system are formulated. Here, a typical surveillance mission as in Figure 3 is considered.

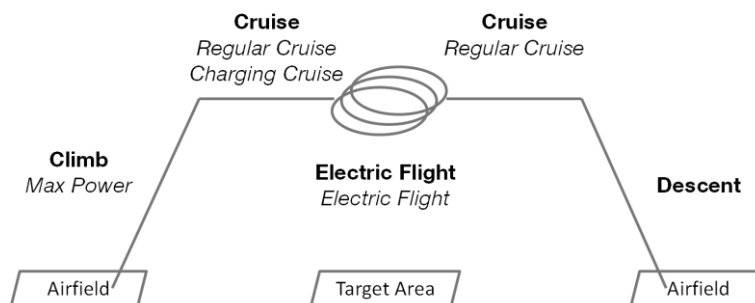


Figure 3: Typical hybrid-electric propulsion surveillance mission with flight phases and design points [20]

The mission starts with takeoff and climb. The takeoff is here neglected, as the energy demand during this phase is highly dependent on the available runway length and very often unmanned aircraft use takeoff auxiliaries as catapults or winches to reduce the takeoff energy demand to a minimum. The cruise phase is divided in two segments, one to the target area, and one from the target area to the landing zone. Over the target area, an electric loiter phase is set. Descent may be neglected, as for low altitude it may be conducted unpowered. The mission may also contain several electric flight phases and cruise phases in which the batteries are recharged.

From the typical mission phases, the four design points indicated in Figure 3 are derived. The maximum power demand occurs during climb. The design point defining this state is consequently labeled *Maximum Power*. In cruise, the internal combustion engine propels the aircraft. The according design point is labeled *Regular Cruise*. In case the batteries are charged during cruise, the engine also drives the electric motor. The design point defining the requirements for this state is named *Charging Cruise*. The requirements for the electric flight are defined in the design point of the same name *Electric Cruise*. Table 1 summarizes the flight phases, the activities of the internal combustion engine (ICE) and the electric motor (EM) as well as the design points and the degree of hybridization. The degree of hybridization (DoH) is a figure to describe the interaction between electric motor and internal combustion engine. It stands for the fraction of propeller shaft power delivered by the electric motor. Consequently it takes the value 1 during *Electric Flight* and 0 during *Regular Cruise*. These points are the single-mode design points, because only one machine works isolated. The design points *Charging Cruise* and *Maximum Power* are called dual-mode points, because the two machines interact. During the former, the DoH is below zero, as energy is fed into the electric system. At the *Maximum Power* design point, the DoH may lie between 0 and 1.

Table 1: Flight phases, ICE and EM activities and design points of a surveillance mission

Flight Phase	ICE activity	EM activity	Design Point	Degree of Hybridization
1 Climb	drives propeller jointly with EM	drives propeller jointly with ICE	<i>Maximum Power</i>	$0 < \text{DoH} < 1$
2 Cruise	drives propeller and EM	Acts as generator to charge batteries	<i>Charging Cruise</i>	$\text{DoH} < 0$
3 Electric Flight	inactive	Drives propeller	<i>Electric Flight</i>	$\text{DoH} = 1$
4 Cruise	Drives propeller	Inactive	<i>Regular Cruise</i>	$\text{DoH} = 0$
5 Descent	inactive	Inactive	None	not applicable

The propulsion system design procedure is based on the use of state variables, the only exception being the internal combustion engine input power. The inputs of the process are hence the state variables for propulsion power, thrust and velocity, and flight time, which is required to size the energy storages. All inputs must be given for each of the four design points. The output is the propulsion system mass. Figure 4 shows the process in the form of the different included modules and their input and output variables.

For almost every component in the powertrain mass and efficiency are computed from the output power state variables and the design variables. The exceptions are the coupling and the fuel tank. For the fuel tank only mass is computed, whereas no energy dissipation is modeled. The coupling in preliminary design is neglected in mass and efficiency, as its realization is depending on the mechanical concept and may be regarded in detail in a later design phase. The 15 possible design variables summarized in the center box in Figure 4 are characteristic properties of the respective component.

The design process is backward-facing, which means that it runs from the propeller to the energy storages, contrary to the direction of physical energy flow. A backward-facing process runs faster than a forward-process, because compliance with the preset performance requirements, here the propeller output power state variables, is guaranteed in every run. In a forward-facing process, initial assumptions for the energy storages and power converters need to be adjusted until compliance is reached. This results in an iterative and more time-consuming process. As a disadvantage, the backward-facing process makes the inclusion of some detailed models impossible, e.g. energy storage polarization curves. In the course of the process, first the propeller is sized, then the energy converters and finally the energy storages. The procedure includes models for propellers; couplings; internal combustion engines, electric motors, electronic speed controllers; batteries; and fuel tanks. All of these models except for the coupling are described in chapter 5. The coupling is assumed to be a pulley assembly, as in realized parallel hybrid-electric systems [8, 12]. It is modeled with a coupling constant, the ratio of the pulley radii, which governs the distribution of torque and rotational velocity on the electric path and the combustion engine path.

If the process is run within an optimization framework, the objective is to minimize the propulsion system mass by modifying the design variables.

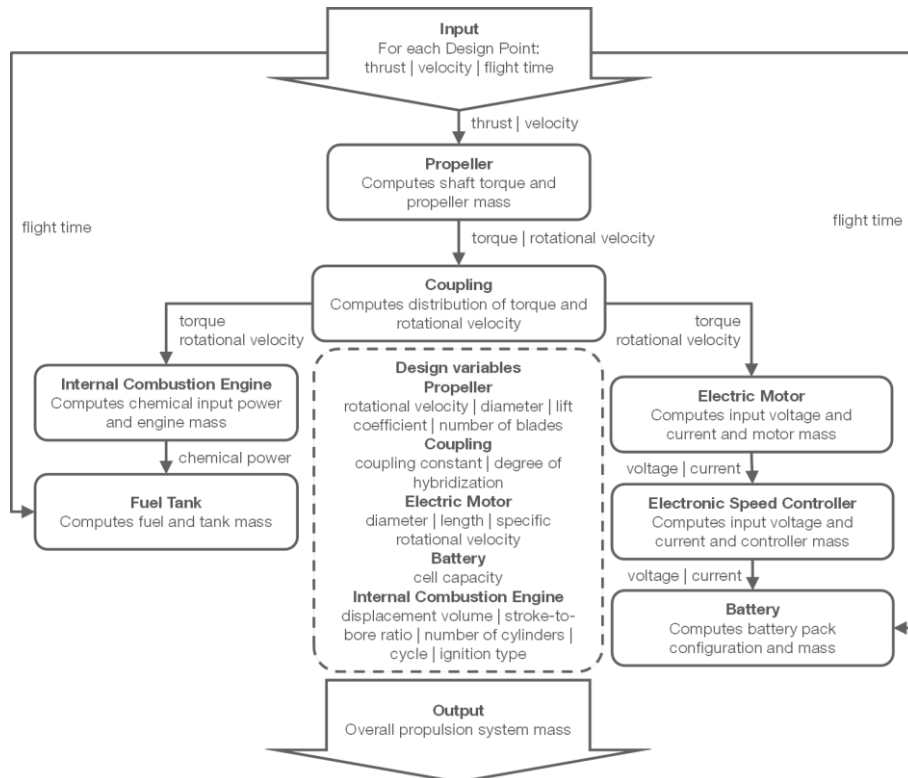


Figure 4: Parallel hybrid-electric propulsion system design procedure (modified from [19])

5. Modeling of the components of hybrid-electric propulsion systems

Baseline models for all of the regarded components are described in [19], so that here only enhancements are explained in detail. Significant changes were included into the electric motor model, which, in its previous form, was only applicable to a very limited design space. Furthermore, models to estimate the internal resistance of the motor controller and battery were incorporated.

5.1 Propeller model

The propeller model returns efficiency, torque and rotational velocity for an input of the design variables and the propulsion power state variables thrust and velocity. Due to the complexity of propeller aerodynamics, the existing tool XROTOR¹ was used. The propeller data is computed outside of the design procedure due to the high required computational time. The data is then included into the process by interpolation.

The tool optimizes propeller blade chord and twist distribution for one propeller design point, defined by thrust, velocity, lift coefficient, rotational velocity and diameter. Additionally to the propeller design point, not to be confused with the propulsion design points in chapter 4, the model output is computed for so-called propeller off-design points. The propeller off-design points are other operational requirements in terms of thrust and velocity to the propeller optimized for the propeller design point. In the process, the operational data for the propeller design points (thrust and velocity) are taken from the propulsion design points with the longest flight time. The requirements at the other propulsion design points define the propeller off-design points.

A propeller mass model is taken from [26]. It was validated for small CFRP propellers in [6].

¹ Available at <http://web.mit.edu/drela/Public/web/xrotor/> [Accessed 22 May 2013]

5.2 Electric motor model

Figure 5 shows the electric motor design procedure. Its input consists of the operational variables and the design variables. The operational variables, according to Figure 4, are the state variables for shaft power, torque and rotational speed. The choice of the design variables is explained later. The model's outputs are the input voltage and current as well as motor mass.

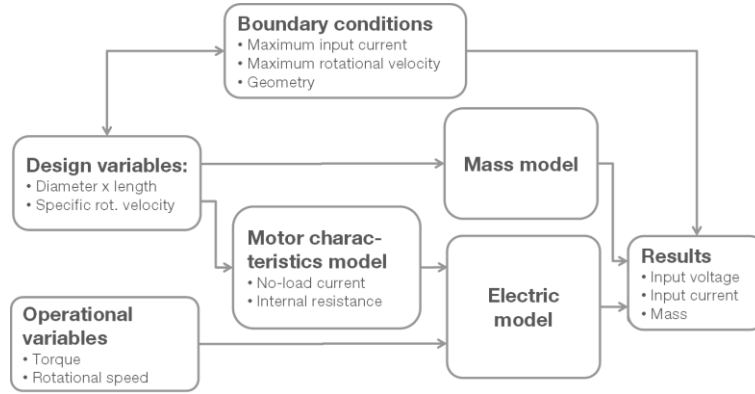


Figure 5: Electric motor design procedure (modified from [20])

The electric model is derived from a surrogate circuit [19, 25]. It uses three motor characteristics: internal resistance R_i , no-load current I_0 and specific rotational velocity K_v . Those three characteristics are generically determined from the design variables. The surrogate model to do so is derived from a database of over 700 brushless DC motors. Due to the limited published data of these commercial motors, the possible design variables are reduced to diameter, length and number of windings. As the number of windings is an absolute value of low informative value if no other data are given, the specific rotational velocity is used as design variable [19]. The original motor characteristics surrogate model is fit using a two-dimensional power function based on the 275 inrunner motors of manufacturer Lehner² [19]. The function returns significantly too low internal resistances for high dl , so that another approach using the same data was developed. It makes use of the fact that the curves of R_i and I_0 over K_v are very similar for each motor series. A motor series is a group of motors with the same diameter and length. When fit, each curve may be described in the form given in (1) and (2) with very high accuracy.

$$R_i = c_{Ri} K_v^{-2} \quad (1)$$

$$I_0 = c_{I0} K_v^{1.63} \quad (2)$$

The coefficients c_{I0} and c_{Ri} may then be determined with power fits over dl as shown in Figure 6. The new model allows the inclusion of larger motors and returns more accurate results, especially for the internal resistance. The mass model also was derived from the motor database. It is a linear function of only one independent variable. More accurate results are obtained using the product of the square diameter and length d^2l , whereas the use of the product of diameter and length dl reduces computational time. If the function's argument is d^2l , both diameter d and length l need to be used as design variables. The resulting increase in computational time is set in comparison the gain in accuracy in chapter 6.1. The function of dl is plotted with the original data in Figure 7.

² Data available at <http://www.lehner-motoren.de> [Accessed 17 May 2013]

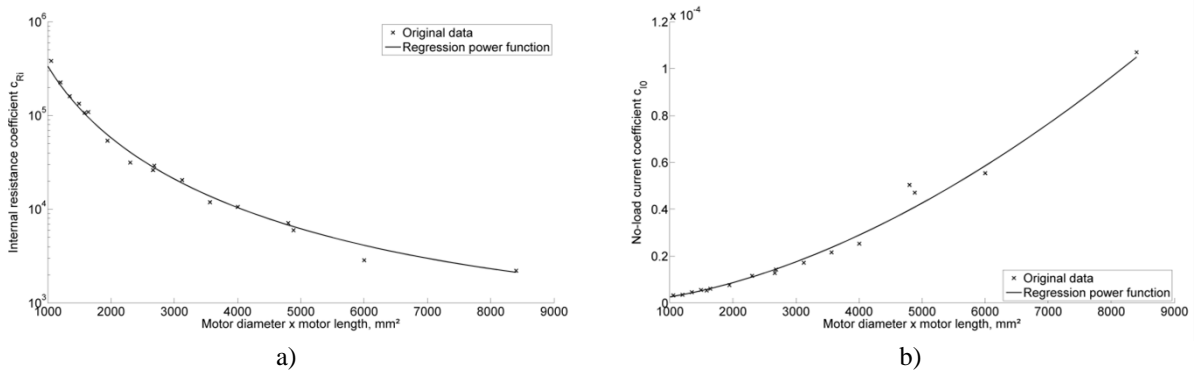


Figure 6: Coefficients for the estimation of electric motor characteristics a) internal resistance b) no-load current

For the electronic speed controller, a mandatory auxiliary device for brushless direct-current motors, efficiency estimation from [6] was re-formulated for the use in a backward-facing procedure. Imperfect efficiency appears in the form of a voltage drop. The efficiency estimation bases on experimental data. As only three commercial controllers were measured, the data of one model is used generally [6]. In Figure 7, the efficiency map of the electronic speed controller is given as function of the power fraction and input voltage.

The mass of the electronic speed controller is estimated using a fit derived from a database of 50 commercial electronic speed controllers [19].

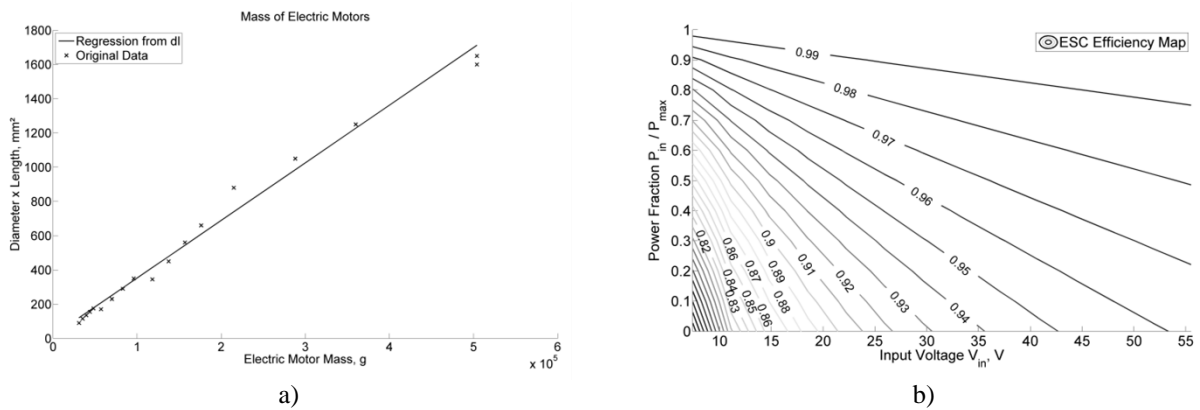


Figure 7: a) Mass estimation for the electric motor and b) Efficiency map of the electronic speed controller

5.3 Battery model

The battery model described by the authors in [19] distinguishes itself from existing battery mass estimations by returning not only mass, but also the battery layout in cells in series or parallel. The input data are the voltage and current required by the electronic speed controller and flight time. The battery design variable is the cell capacity. For the analysis in this paper the model was amended with an estimation of the battery's internal resistance, based on the model in [6]. There, resistance is computed as a function of the battery c-rate and capacity. The model was applied to a database with 400 commercial Lithium-polymer batteries and a one-dimensional power function of cell capacity was fitted to the results as plotted in Figure 8. With the internal resistance, the required open-circuit voltage of the battery is computed from its required output voltage using Ohm's law. Then the number of cells in series is determined using a nominal cell voltage of 3.7 V for Lithium-polymer batteries. The number of cells in parallel is the required capacity divided by cell capacity. It is assumed, that only 80 % of the battery's capacity may be used without causing damage to it [6]. An estimation of battery mass as function of energy content and maximum continuous discharge current was derived from the database of COTS batteries [19].

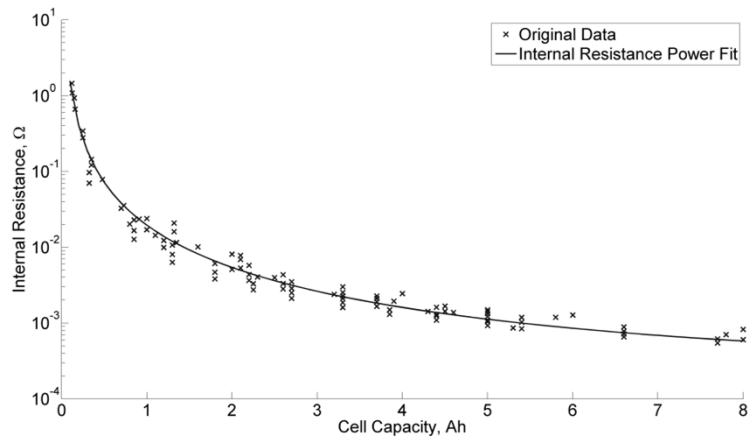


Figure 8: Battery internal resistance estimation

5.4 Internal combustion engine model

The internal combustion engine model is described in detail in [19]. It returns the required chemical power and the engine mass for inputs including the state variables for the shaft power, torque and rotational speed, and the design variables. The design procedure is shown in Figure 9.

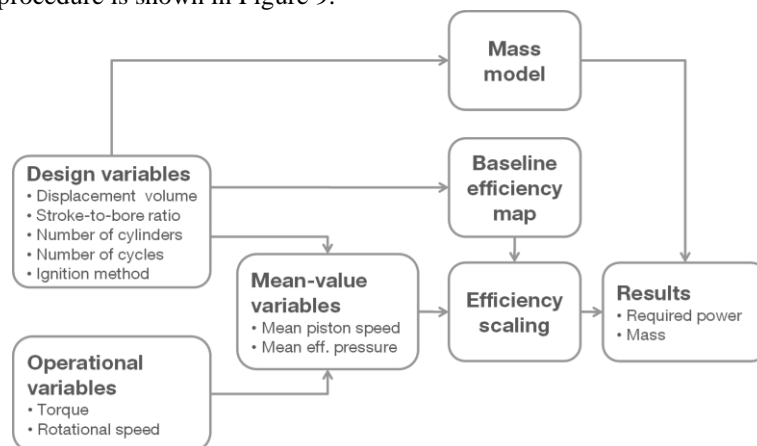


Figure 9: Internal combustion engine design procedure (modified from [20])

To return the chemical power, the engine efficiency is determined. The model scales an existing engine efficiency map. For scaling purposes it is recommended to use mean-value variables instead of the absolute operational variables torque and rotational velocity [27]. To convert the operational variables into mean-value variables, the displacement volume and the cylinder stroke are required. Instead of the stroke, the relative stroke-to-bore ratio is chosen as design variable together with the displacement volume, the number of cylinder, the cycle and the ignition method. The last three variables are used to choose a baseline efficiency map suitable for the target engine. The baseline efficiency map is formulated in a normalized form, so that it can be scaled to the target engine. The scaling process was validated with published wide-open throttle curves of COTS multi-purpose engines [19]

The engine mass prediction model was a linear function of displacement volume fitted to a database of over 250 small commercial internal combustion engines with displacement volumes below 420 cm³ [19].

5.5 Fuel tank model

The fuel tank model's input is the chemical power required by the engine. It returns mass of the fuel and the fuel tank. The fuel system is assumed to be an ideal system, so no power loss is modeled, and the formulation in state variables is not necessary. The mass and the volume of the required fuel are determined using the gravimetric density and the specific power of the used fuel. The fuel tank mass estimation function is derived from a database of 40 commercial tanks [19].

6. Propulsion system analysis

6.1 Computational restrictions of the design process

The selection of an optimum propulsion system in this chapter is conducted using full-factorial iteration. This means the design procedure is run for each combination of the design variables. In Figure 4, 15 possible design variables are listed. Of those, the engine cycle and ignition type are limited to 2 values (two-stroke and four-stroke; spark-ignition and compression-ignition) and may be set before the process is run. The same may be applied for the number of engine cylinders and the number of propeller blades, which also only may take a limited number of values. If a range of 5 support points was explored for each of the remaining 11 design variables, this would result in 5^{11} or almost 49 million combinations and consequently calls of the design procedure. If the computation time for one run could be reduced to one second, it still would take more than 80 weeks to generate the results. Therefore, the number of design variables needed to be restricted further. The stroke-to-bore ratio of the internal combustion engine and the propeller lift coefficient were hence set to constant values. Furthermore the merge of two design variables, electric motor diameter d and length l , into one, the product of diameter and length dl , was assessed. The mean relative difference in propulsion system mass computed was below 1 % and negligible, whereas the computation time could be significantly reduced by 93 %. In addition, the hybrid-electric design procedure with design variables d and l could not be run on a state-of-the-art COTS computer with 64-bit operating system and 8 GB memory.

6.2 Analysis procedure

Three propulsion system types are compared in this chapter

- Internal combustion engine propulsion system
- Battery-electric propulsion system
- Hybrid-electric propulsion system

In order to quantify their differences, an exemplary surveillance mission is provided. The mission for the hybrid-electric system is depicted in Figure 3. For the conventional propulsion types, conventional here being defined as non-hybrid, distinguishing between cruise and electric flight is not reasonable. A battery-electric aircraft per se flies electrically, whereas the combustion engine aircraft is not capable of flying electrically. The mission hence may be simplified to the one given in Figure 10. The number of design points is then reduced to two: *Maximum Power* and *Regular Cruise*.

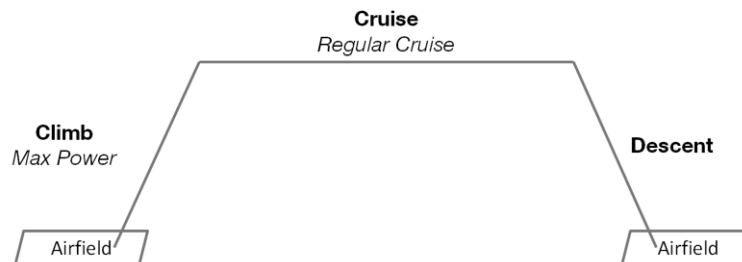


Figure 10: Typical conventional propulsion surveillance mission with flight phases and design points ([20])

The hybrid-electric system is analyzed using the process described in chapter 4. For the battery-electric system and the combustion engine system, the modules of the process are re-arranged. Following the propeller module, either the electric path with electric motor, motor controller and battery modules is run for the battery-electric system or the internal combustion engine and fuel tank module for the combustion engine system. For the battery-electric system the electric motor gear ratio was introduced as an additional design variable.

The required input to run the process described in chapter 4 is thrust, velocity and flight time for each design point. For this analysis, the flight time, thrust and velocity for the design point *Regular Cruise* (RC) are set. The *Maximum Power* (MP) thrust T_{MP} can be computed according to (3) from the velocities at *Maximum Power* v_{MP} and *Regular Cruise* v_{RC} , the *Regular Cruise* thrust T_{RC} , the rate of climb *RoC* and the aerodynamic efficiency at cruise $L/D|_{RC}$. The equation is based on the assumption that the aircraft is climbing with constant rate of climb and has constant aerodynamic efficiency at cruise.

$$T_{MP} = T_{RC} \left[\left(\frac{v_{MP}}{v_{RC}} \right)^2 + \frac{L}{D}_{RC} \frac{RoC}{v_{MP}} \right] \quad (3)$$

In order to keep the analysis concise, the number of degrees of freedom in the requirements is kept as low as possible. The velocity at *Maximum Power* v_{MP} is therefore set equal to the velocity at *Regular Cruise* v_{RC} . Further values are set globally: The rate of climb RoC to 3 m/s and altitude to 900 m. This leads to a *Maximum Power* flight time of 5 min. A lift-to-drag ratio L/D_{RC} of 10 is a reasonably conservative assumption for an aircraft with antennae and camera or other equipment mounts. For the analysis of the hybrid-electric propulsion system, also the requirements for the design point *Electric Flight* (EF) must be quantified. Velocity v_{EF} again is set equal to v_{RC} , so that also the thrust equals that in *Regular Cruise*. The electric flight time has, as will be shown later, a significant influence on the mass of hybrid-electric propulsion systems. It is here set to 25 % of the overall flight time.

This analysis is conducted twofold.

1. In the first part, a so called requirement space is defined by two thrust levels and reasonable ranges of cruise velocity and endurance for each. For all three propulsion types, the propulsion system mass is then computed over the defined requirement space.
2. In the second part, thrust and velocity are kept constant and only flight time is varied. This reduction allows taking a detailed look into the system properties.

For part one, *Regular Cruise* thrust levels of 20 N and 100 N are chosen. Common ranges for velocity and flight time were derived from the unmanned aircraft databases in [1] and [28]. Velocities are investigated from 20 m/s to 65 m/s and flight times from 1 h to 24h. For part two of the analysis, the characteristics of the Institute of Aircraft Design's research aircraft IMPULLS³ are used as a baseline. This means a cruise thrust of 20 N and cruise velocity of 20 m/s. The data are regarded at flight times of 1.5 h, 12 h and 24 h.

6.3 Internal combustion engine propulsion system

Figure 11 shows the mass of internal combustion engine propulsion systems at the two thrust levels 20 N and 100 N and varying cruise velocities from 20 m/s to 65 m/s and varying flight times from 1 h to 24h. Mass increases with increasing velocity and flight time, as the power demand behaves proportional with velocity and the energy demand with velocity and flight time.

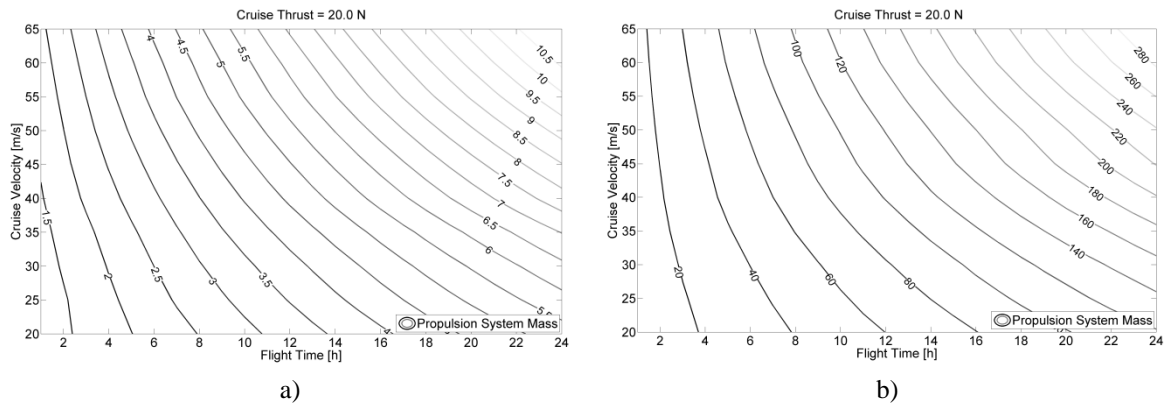


Figure 11: Mass of internal combustion engine propulsion systems at different cruise thrust levels: a) 20 N b) 100 N

Table 2 summarizes the data for a propulsion system with cruise thrust of 20 N and cruise velocity of 20 m/s. The data show the increasing importance of efficiency with flight time. The higher the required flight time is, the heavier is the energy storage. The required energy in the storage, which is proportional to its mass, is a linear function of the system efficiency. Therefore efficiency is increased, even at the expense of heavier energy converters, when the decrease in storage mass exceeds the increase in converter mass. For the 12 h case, in comparison to the 1.5 h case, a bigger but slower rotating propeller is selected. This increases the propeller efficiency, whereas the lower rotational velocity causes a higher torque demand to the internal combustion engine. Therefore a bigger displacement volume is selected and the engine consequently is heavier.

³ Data available at <http://www.lls.mw.tum.de/index.php?id=33#c432> [Accessed 17 May 2013]

The combustion engine propulsion system may be used to visualize the so called propulsion system design dilemma. In the efficiency map of the 22.9 cm³ engine used in the 12 h case in Figure 12, the *Maximum Power* and the *Regular Cruise* design point are indicated. High efficiencies are obtained for high torque demands and therefore the difference in torque between *Maximum Power* and *Regular Cruise* limits the efficiency for the latter design point to an unfavorably low value, although it accounts for over 99 % of the flight time.

Table 2: Data of combustion engine propulsion systems with cruise thrust of 20 N and at a velocity of 20 m/s

	Flight time 1.5 h	Flight time 12 h	Flight time 24 h
<i>Masses [kg]</i>			
System	1.32	3.21	5.27
ICE	0.83	0.92	0.92
Fuel & tank	0.37	2.16	4.22
Propeller	0.12	0.13	0.13
<i>Internal Combustion Engine</i>			
Efficiency (Regular Cruise / Max Power)	0.25 / 0.32	0.28 / 0.34	0.28 / 0.34
Displacement Volume [cm ³]	20.6	22.9	22.9
<i>Propeller</i>			
Rotational Velocity [rpm]	5500	4000	4000
Tip Radius [m]	0.25	0.30	0.30
Efficiency	0.77 / 0.70	0.8 / 0.75	0.8 / 0.75

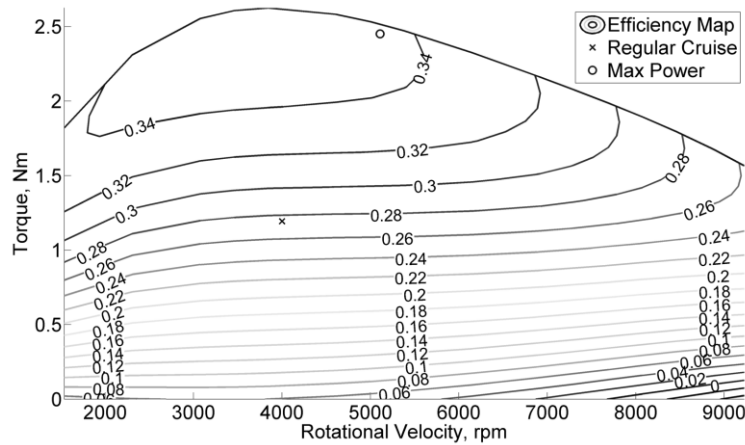


Figure 12: Efficiency map of the internal combustion engine in a combustion engine propulsion system with requirements 20 N, 20 m/s, 12 h

6.4 Battery-electric propulsion system

Figure 13 shows the mass of battery-electric propulsion systems for the two thrust levels. The battery-electric systems are significantly heavier than the combustion engine systems designed for the same requirements, whereas the course of mass over flight time and velocity is very similar. For some requirement combinations the propulsion system mass significantly exceeds the value feasible in a 150 kg aircraft, the maximum takeoff mass this method was designed for.

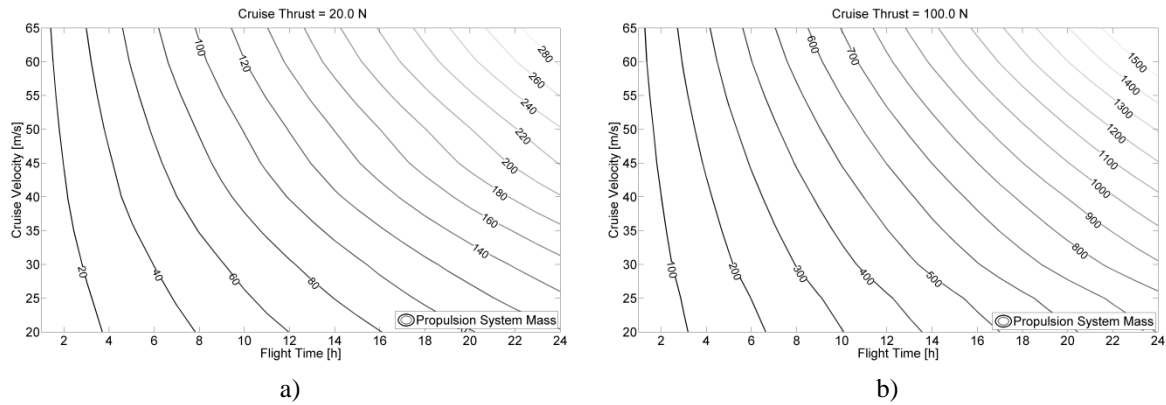


Figure 13: Mass of battery-electric propulsion systems at different cruise thrust levels: a) 20 N b) 100 N

The detailed data for the 20 N and 20 m/s cases in Table 3 show the high percentage of battery mass in the system mass. For the 1.5 h case it accounts for 92 % of the system mass, for the 24 h case even 99 %. The increasing importance of efficiency for high endurance systems stated for the combustion engine systems is also visible for the battery-electric system. Higher efficiencies are obtained with bigger and slower rotating propellers at the expense of bigger motors for the increased torque demand. The efficiencies of the electric motor in the two design points are nevertheless significantly closer to each other, so that the propulsion system design dilemma does not affect battery-electric propulsion systems as strong as combustion engine systems.

Table 3: Data of battery-electric propulsion systems with cruise thrust of 20 N and at a velocity of 20 m/s

	Flight time 1.5 h	Flight time 12 h	Flight time 24 h
<i>Masses [kg]</i>			
System	9.30	60.18	118.44
Electric motor	0.61	0.96	0.96
Electronic speed controller	0.04	0.04	0.04
Battery	8.51	59.03	117.29
Propeller	0.14	0.15	0.15
<i>Electric Motor</i>			
Efficiency (Regular Cruise / Max Power)	0.94 / 0.94	0.94 / 0.94	0.94 / 0.94
Diameter x Length [mm ²]	3600	5150	5150
Specific Rotational Velocity	458	300	300
Gear ratio	5	5	5
<i>Propeller</i>			
Rotational Velocity [rpm]	3000 / 3780	2000 / 2490	2000 / 2490
Tip Radius [m]	0.35	0.35	0.4
Efficiency	0.82 / 0.78	0.85 / 0.81	0.85 / 0.81

6.5 Hybrid-electric propulsion system

In Figure 14, the hybrid-electric propulsion system masses for the two thrust levels are compared. Masses are between those of the battery-electric and the combustion engine systems. A quantitative assessment is highly dependent on the percentage of electric flight time and therefore only reasonable for a specific use case.

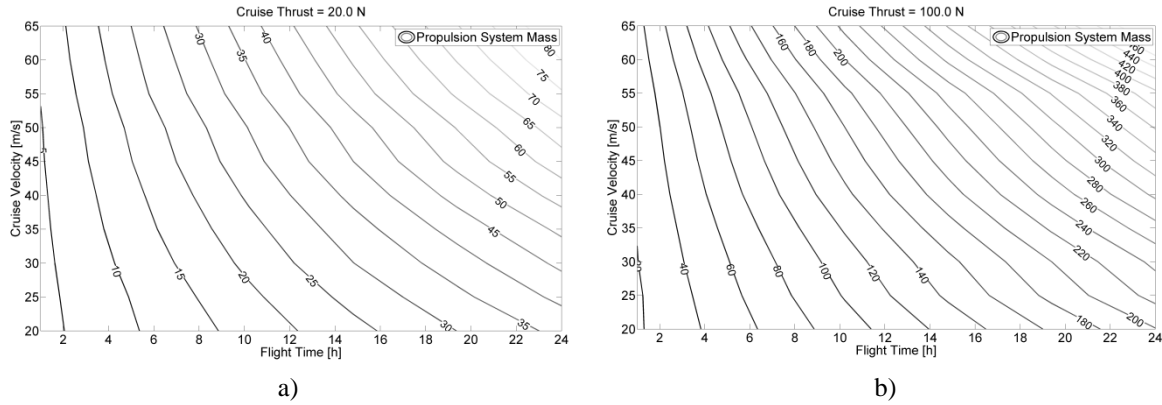


Figure 14: Mass of hybrid-electric propulsion systems at different cruise thrust levels: a) 20 N b) 100 N

The investigated flight times for the hybrid-electric propulsion system include one quarter of electric flight time each. For the three cases summarized in Table 4 this results in 22.5 min of 1.5 h, 3 h of 12 h and 6 h of 24 h. The energy converters used as primary motive power units in the conventional systems may be downsized in the hybrid-electric system. This is the case for the internal combustion engine in all three cases. The electric motor for the 24 h case is the same size of that in the battery-electric system, the other two are smaller. With increasing flight time the trend to use slower rotating, bigger diameter propellers described for the conventional systems is also observable in the results for the hybrid-electric system. Furthermore, the so called propulsion system design dilemma is solved by the hybrid-electric propulsion system, as the efficiency at the *Regular Cruise* design point for the internal combustion engine and at the *Electric Flight* design point for the electric motor are very close to or even higher than the *Maximum Power* efficiency. The difference in efficiency between the two design points (*EF* and *MP* for the electric motor; *RC* and *MP* for the internal combustion engine) is driven by the difference in power demand. It is set by the degree of hybridization at *Maximum Power*, the only dual mode design point regarded in this analysis. For the 1.5 h and 12 h case power is evenly divided to the two machines, for 24 h case the electric motors delivers 60 %. The coupling constant, equivalent to an electric motor gear ratio, decreases with increasing flight time. This runs analogously with a decrease in rotational velocity and electric motor specific rotational velocity.

Table 4: Data of hybrid-electric propulsion systems with cruise thrust of 20 N and at a velocity of 20 m/s

	Flight time 1.5 h	Flight time 12 h	Flight time 24 h
<i>Masses [kg]</i>			
System	4.03	19.35	36.37
Electric motor	0.26	0.61	0.96
Electronic speed controller	0.03	0.03	0.03
Battery	2.93	16.70	32.07
Internal Combustion Engine	0.47	0.57	0.65
Fuel & tank	0.23	1.32	2.53
Propeller	0.11	0.12	0.13
<i>Coupling</i>			
Degree of Hybridization (<i>MP</i>)	0.5	0.5	0.6
Coupling Constant	3	2.5	2
<i>Electric Motor</i>			
Efficiency (<i>EF</i> / <i>MP</i>)	0.93 / 0.93	0.93 / 0.93	0.93 / 0.94
Diameter x Length [mm ²]	2050	3600	5150
Specific Rotational Velocity	849	383	247
<i>Internal Combustion Engine</i>			
Efficiency (<i>RC</i> / <i>MP</i>)	0.34 / 0.33	0.35 / 0.34	0.35 / 0.33
Displacement Volume [cm ³]	10.8	13.7	15.7

Propeller

Rot. Velocity [rpm] (<i>RC / EF / MP</i>)	8000 / 8000 / 10520	5000 / 5000 / 6470	4000 / 4000 / 5110
Tip Radius [m]	0.2	0.25	0.3
Efficiency (<i>RC / EF / MP</i>)	0.72 / 0.72 / 0.64	0.77 / 0.77 / 0.70	0.80 / 0.80 / 0.75

7. Conclusion and outlook

This paper describes a procedure for the design of hybrid-electric propulsion systems for small-unmanned aircraft that fulfils three demands: high accuracy, fast computation time and generality. The procedure is composed of several component models, for which several enhancements to an earlier published version are described. An improvement of the surrogate model for electric motor characteristics enables the modelling of a bigger range of electric motors. For the electronic speed controller and the battery, power losses were included. Several trends become visible in the comparison of the hybrid-electric propulsion system with two conventional systems, the battery-electric and the combustion engine system. The internal combustion engine and the electric motor in a hybrid-electric propulsion system may be downsized compared to the system in which they act as primary motive power unit. Especially for the internal combustion engine, the efficiency for the cruise phase may be significantly increased, as the maximum power demand decreases due to a dual use of both machines. The mass of the hybrid-electric system is highly dependent on the electric flight time. The biggest driver for mass in all electric propulsion systems is the battery. A wider applicability of electric propulsion system in aircraft requires an increase of battery specific energy. A prognosis on this parameter sees values of 400 Wh/kg for future Lithium-ion technology and up to 1000 Wh/kg for Lithium-air batteries [29]. The hybrid-electric propulsion system is a transition technology that allows the combination of silent flight phases with phases with high demands in power or energy. A possibility to allow longer electric flight times without mass increase is the inclusion of mission phases in which the batteries are charged by the combustion engine.

Acknowledgements

Parts of the work described in this paper was done by Technische Universität München as subcontractor of Cassidian within the project DemUEB Phase 3 (Demonstration of the use of UAV in Bavaria) funded by the Bavarian Ministry of Economic Affairs, Infrastructure, Transport and Technology (German: Bayerisches Staatsministerium für Wirtschaft, Infrastruktur, Verkehr und Technologie).

References

- [1] Gundlach, J., 2012. *Designing Unmanned Aircraft Systems – A comprehensive approach*, 1st ed., Reston: American Institute of Aeronautics and Astronautics
- [2] Hirling O. and Holzapfel, F., 2012. State of the Art UAS Airworthiness Regulations in Contrast to Alternative Certification Methods. In: *6th UAV World*. Frankfurt am Main, Germany, 6-8 November 2012
- [3] Rizzoni, G., Guzzella, L., Baumann, B.M., 1999. Unified Modeling of Hybrid Electric Vehicle Drivetrains. *IEEE/ASME Transaction on Mechatronics*, 4 (3), pp. 246-256.
- [4] Harmon, F.G., 2005. *Neural Network Control of a Parallel Hybrid-Electric Propulsion System for a Small Unmanned Aerial Vehicle*. Ph.D. University of California Davis
- [5] Hung, J. Y., Gonzalez L.F., 2012a. Design, Simulation and Analysis of a Parallel Hybrid Electric Propulsion System for Unmanned Aerial Vehicles, In: *28th International Congress of the Aeronautical Sciences*, Brisbane, Australia, 2012
- [6] Rößler, C. O., 2011. *Conceptual Design of Unmanned Aircraft with Fuel Cell Propulsion System*. Ph.D. Technische Universität München.
- [7] Noth, A., 2008. *Design of Solar Powered Airplanes for Continuous Flight*. Ph.D. ETH Zürich.
- [8] Ausserer, J. K., Harmon, F. G., 2012. Integration, Validation, and Testing of a Hybrid-Electric Propulsion System for a Small Remotely-Piloted Aircraft. In: *10th International Energy Conversion Engineering Conference*, AIAA, Atlanta, GA, 2012
- [9] Harmon, F. G., Frank, A. A., Chattot, J.-J., 2006. Conceptual Design and Simulation of a Small Hybrid-Electric Unmanned Aerial Vehicle. *Journal of Aircraft*, 43 (5), pp. 1490-1498.
- [10] Hiserote, R., Harmon, F. G., 2010. Analysis of Hybrid-Electric Propulsion System Design for Small Unmanned Aircraft Systems In: *8th Annual International Energy Conversion Engineering Conference*, AIAA, Nashville, TN, 2010.

- [11] Greiser, C. M., Mengistu, I. H., Rotramel, T. A., Harmon, F. G., 2011. Testing of a Parallel Hybrid-Electric Propulsion System for use in a Small Remotely-Piloted Aircraft. In: *9th Annual International Energy Conversion Engineering Conference*, AIAA, San Diego, CA, 2011.
- [12] Glasscock, R., Hung, J. Y., Gonzalez, L. F., Walker, R. A., 2007. Design, Modelling and Measurement of Hybrid Powerplant for Unmanned Aerial Systems (UAS). In: *5th Australasian Congress on Applied Mechanics*, Brisbane, Australia, 2007.
- [13] Glasscock, R., Hung, J. Y., Gonzalez, L. F., Walker, R. A., 2009. Multimodal Hybrid Powerplant for Unmanned Aerial Systems (UAS) Robotics. In: *24th Bristol International Unmanned Air Vehicle Systems Conference*, Bristol, United Kingdom, 2009.
- [14] Hung, J.Y., Gonzalez, L.F., 2012. On parallel hybrid-electric propulsion system for unmanned aerial vehicles. *Progress in Aerospace Sciences*, 51 (2012), pp. 1-17
- [15] Lieh, J., Spahr, E., Behbahani, A., Hoying, J., 2011. Design of Hybrid Propulsion Systems for Unmanned Aerial Vehicles. In: *47th AIAA/ASME/SAE/ASEE Joint Propulsion Conference & Exhibit*, San Diego, CA, 2011.
- [16] Koster, J. et al., 2011. Hybrid Electric Integrated Optimized System (HELIOS) – Design of a Hybrid Propulsion System for Aircraft. In: *49th AIAA Aerospace Sciences Meeting including the New Horizons Forum and Aerospace Exhibition*, Orlando, FL, 2011.
- [17] Deschenes, A., Brown, K., Sobin, A., West, G., 2011. Design, Construction, and Testing of RC Aircraft for a Hybrid Propulsion System. *49th AIAA Aerospace Sciences Meeting including the New Horizons Forum and Aerospace Exhibition*, Orlando, FL, 2011.
- [18] Bagassi, S., Bertini, B., Francia, D., Persiani, F., 2012. Design Analysis for Hybrid Propulsion. In: *28th International Congress of the Aeronautical Sciences*, Brisbane, Australia, 2012
- [19] Schoemann, J., Hornung, M., 2012. Modeling of Hybrid-Electric Propulsion Systems for Small Unmanned Aerial Vehicles. In: *12th AIAA Aviation Technology, Integration and Operations (ATIO) and 14th AIAA/ISSMO Multidisciplinary Analysis and Optimization (MAO) Conference*, Indianapolis, IN, USA, 17-19 September 2012
- [20] Schoemann, J., 2012. DemUEB Phase 3 Abschlussbericht zu WP3911. Technical Report LS-TB-12/07 Technische Universität München
- [21] Lundström, D., Amadori, K., Krus, P., 2010. Validation of Models for Small Scale Electric Propulsion Systems. *48th AIAA Aerospace Sciences Meeting including the New Horizons Forum and Aerospace Exhibition*, Orlando, FL, 2010.
- [22] Gur, O., Rosen, A., 2009a. Optimization of Propeller Based Propulsion System. *Journal of Aircraft*, 46 (1), pp. 95-106.
- [23] Gur, O., Rosen, A., 2009b. Optimization of Electric Propulsion Systems for Unmanned Aerial Vehicles. *Journal of Aircraft*, 46 (4), pp. 1340-1353.
- [24] McElroy, T., Landrum, D. B., 2012. Simulated High-Altitude Testing of a COTS Electric UAV Motor. In: *50th AIAA Aerospace Sciences Meeting including the New Horizons Forum and Aerospace Exhibition*, Nashville, TN, 2012.
- [25] Drela, M., 2007. First-Order DC Electric Motor Model. MIT Aero & Astro.
- [26] Keidel, B., 2000. *Auslegung und Simulation von hochfliegenden, dauerhaft stationierbaren Solardrohnen*. Ph.D. Technische Universität München.
- [27] Guzzella L., Onder C., 2010. *Introduction to Modeling and Control of Internal Combustion Engine Systems*, 2nd ed., Berlin: Springer Verlag
- [28] UVS International, 2012. Remotely Piloted Aircraft Systems – The Global Perspective 2012/2013. [online] Available at: <<http://www.uvs-info.com/>> [Accessed 13 November 2012]
- [29] Christensen, J. et al., 2012. A Critical Review of Li/air Batteries. *Journal of the Electrochemical Society*, 159 (2), pp. R1-R30